Journal of Physics G:
Nuclear and Particle
Physics

PAPER

New insights into sub-barrier fusion of ^{28}Si + ^{100}Mo

To cite this article: A M Stefanini *et al* 2021 *J. Phys. G: Nucl. Part. Phys.* **48** 055101

IOP Publishing Journal of Physics G: Nuclear and Particle Physics
J. Phys. G: Nucl. Part. Phys. **48** (2021) 055101 (14pp) https://doi.org/10.1088/1361-6471/abe8e2

New insights into sub-barrier fusion of ^{28}Si + ^{100}Mo

A M Stefanini[1,*], G Montagnoli[2], M D'Andrea[2], M Giacomin[2], C Dehman[2], R Somasundaram[2], V Vijayan[2], L Zago[2], G Colucci[2], F Galtarossa[1], A Goasduff[2] and J Grebosz[3]

[1] INFN, Laboratori Nazionali di Legnaro, I-35020 Legnaro (Padova), Italy
[2] Dipartimento di Fisica e Astronomia, Università di Padova, and INFN-Padova, I-35131 Padova, Italy
[3] Institute of Nuclear Physics, Polish Academy of Sciences, PL 31-342 Cracow, Poland

E-mail: alberto.stefanini@lnl.infn.it

Received 7 January 2021, revised 17 February 2021
Accepted for publication 23 February 2021
Published 6 April 2021

Abstract

Fusion cross sections of the ^{28}Si + ^{100}Mo system have been measured near and below the Coulomb barrier by detecting the evaporation residues at forward angles. The excitation function has an overall smoother trend than what obtained in a previous experiment, and a large discrepancy is found for the lowest-energy region, where we observe a tendency of the S factor to develop a maximum, which would be a clear indication of hindrance. The results have been compared with the theoretical prediction of coupled-channels calculations using a Woods–Saxon nuclear potential, and including the low-energy excitation modes of both nuclei. Good agreement with data is found by including, in the coupling scheme, the three lowest members of the ground state rotational band of the oblate deformed ^{28}Si, and two-phonons of the strong quadrupole vibration of ^{100}Mo. The additional coupling, in a schematic way, of the two-neutron pick-up between ground states (Q-value = +4.86 MeV) has a minor effect on calculated cross sections, and does not essentially improve the data fit. The excitation function of ^{28}Si + ^{100}Mo has been compared with that of (1) the heavier system ^{60}Ni + ^{100}Mo having analogous features, and (2) several near-by ^{28}Si, ^{32}S + Zr, Mo systems with various nuclear structures and transfer Q-values. The role of quadrupole and octupole excitation modes, as well as of transfer channels, in affecting the fusion dynamics, are clarified to some extent. Systematic measurements of fusion barrier distributions and CC calculations

*Author to whom any correspondence should be addressed.

properly including transfer couplings, are necessary, in order to shed full light on the influence of the various coupled channels on the fusion cross sections.

Keywords: heavy-ion fusion, sub-barrier cross sections, coupled-channels model, electrostatic beam deflector

(Some figures may appear in colour only in the online journal)

1. Introduction

Heavy-ion fusion in the energy region near and below the Coulomb barrier is well known to be strongly influenced by nuclear structure effects [1–3]. One systematically observes enhancements of the cross sections that arise from couplings of the entrance channel to the low-lying collective modes of the colliding nuclei, such as permanent deformations and surface vibrations. Couplings to nucleon transfer channels are important in many cases as well, as suggested for the first time by Broglia *et al* [4] who pointed out in particular that transfer couplings with $Q > 0$ lead to an enhancement of sub-barrier fusion.

When compared to inelastic excitations, a clear-cut characteristic of transfer reactions is that the Q-value of the reaction may be negative or *positive*, at variance with inelastic excitations. In the CC model [5, 6] fusion barrier distributions (BD) [7] with different shapes are obtained in the two cases, so that contrasting trends of the excitation function are produced, that decreases more slowly with the energy when $Q > 0$, whereas an overall enhancement is produced when $Q < 0$ and the slope does not change appreciably.

However, in spite of the several experimental evidences, reproducing the sub-barrier excitation functions within the coupled-channels (CC) model taking into account transfer couplings quantitatively, is a complex job that only in selected cases (see e.g. reference [8]) has been successfully finalized. In several studies, the 'exact' CC code CCFULL [9] has been employed, that however only allows to include one pair-transfer channel with a macroscopic coupling form-factor as given in reference [10].

Interesting data on ^{32}S + ^{90,96}Zr were obtained by the Beijing group [11, 12] and analysed using the 'empirical coupled channels model' [13] which proved to be very successful in describing these systems and many others where transfer couplings play an important role. A development of this model has been recently performed by Karpov [14] (quantum coupled channels + empirical neutron rearrangement model) producing a good agreement with the BD, besides excitation functions, of several S, Ca + Zr and Ni + Mo cases.

Inelastic collective excitations of different nature (multipolarity) may contribute. Two, three, and possibly multiple phonon vibrations have to be considered, especially in medium-heavy systems, so that the observed BD often have a complex structure giving rise to excitation functions where disentangling the various contributions is not straightforward. An appreciable help may come from the comparison of near-by systems where nuclei possessing different structures are involved.

In this work we have considered the system ^{28}Si + ^{100}Mo whose fusion excitation function was first measured long ago [15]. The cross sections measured in that experiment are reported in figure 1 as blue dots. The excitation function overall appears to be not as smooth as one would expect. In particular, the lowest-energy point is inconceivably low—that cross section being a factor ≈600 smaller than the second-lowest one, with a c.m. energy difference of only 1.7 MeV. This is not plausible, even supposing that fusion hindrance [16, 17] shows up. The inset shows, additionally, an unrealistic glitch around 10 mb.

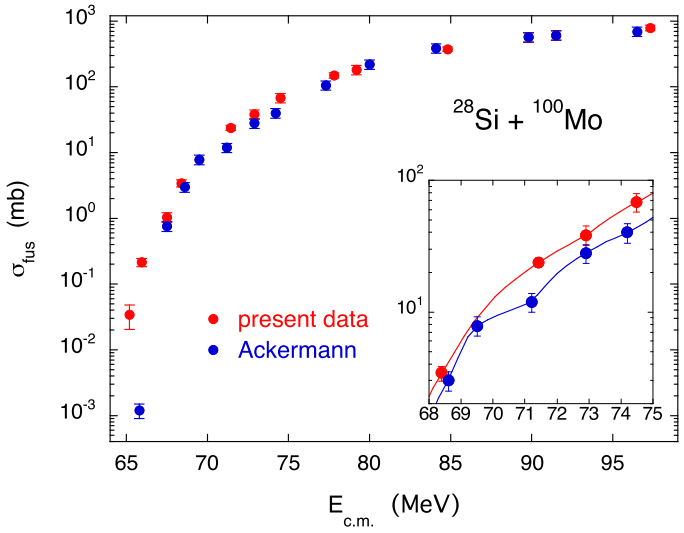

Figure 1. Fusion excitation function of ^{28}Si + ^{100}Mo as measured in the present work (red dots), and as reported in reference [15] (blue dots).The inset shows in particular the cross section region around 10 mb, where an irregularity in the blue dots is observed (please note that the scale is logarithmic). The reported errors are statistical uncertainties. The lines connecting the points are only visual guides.

Further points of interest in the fusion of ^{28}Si + ^{100}Mo come (1) from the permanently deformed oblate shape of ^{28}Si, (2) from the strong quadrupole vibrational nature of ^{100}Mo, and (3) from the existence of several neutron pick-up channels with large and positive ground state to ground state Q-values (see section 3). In the heavier case of ^{60}Ni + ^{100}Mo (studied at Argonne some years go [18]) the situation of transfer channels is quite analogous with many $Q > 0$ available neutron pick-ups, but in spite of this it was observed that they bring a marginal contribution to fusion enhancement below the barrier, whereas the dominant role is played by multi-phonon couplings of the low-lying vibrational collective mode of ^{100}Mo, in the whole measured energy range down to a few μb. This was concluded from the results of CC calculations for that heavier system (see figure 3 of reference [18]), where couplings up to the 4th phonon were found to be necessary to reproduce the data.

Hence we have decided to repeat the measurements on ^{28}Si + ^{100}Mo (with a different set-up) in order to clarify the situation at least from the experimental point of view, because of the several interesting features coexisting in this system.

The results have been compared to the outcomes from the ^{60}Ni + ^{100}Mo experiment. Moreover, since in the mass region of ^{28}Si + ^{100}Mo several other systems display different nuclear structure situations and transfer Q-values, in the last part of this paper the excitation function of ^{28}Si + ^{100}Mo has been compared with that of a number of near-by ^{28}Si, ^{32}S + Zr, Mo cases that were previously investigated. The detailed comparison is useful to clarify the role of strong existing quadrupole and octupole excitation modes, as well as of transfer channels, in affecting the fusion dynamics in that mass region.

We describe in section 2, the experimental set-up and we report the results of the new experiment. The following section 3 gives details of the calculations within the coupled-channel model, and illustrates the comparison with data. The comparison with the fusion data of other systems is performed in section 4 and the whole work is summarized in section 5.

2. Experiment and results

2.1. The set-up

The experiment was performed using the ^{28}Si beam of the XTU Tandem accelerator at the Laboratori Nazionali di Legnaro (LNL) of INFN. A ^{nat}Si metallic sample was used in the sputter ion source. Typical intensities of the accelerated beams were 5–7 pnA with energies in the range 84.0–125.0 MeV. The targets were evaporations of ^{100}Mo (150 μg cm^{-2}) on carbon backings (15 μg cm^{-2}) facing the beam. The target isotopic enrichment was 97.4%; the presence of small amounts of lighter molybdenum isotopes introduced small corrections to the measured ER yields above the barrier, but did not affect the results at lower energies, since ^{100}Mo is the heaviest stable molybdenum isotope, and the Coulomb barriers associated with lighter isotopes are higher. Lower Z contaminations in the targets were unsignificant. The beam energy loss across the carbon backing and half of the ^{100}Mo targets was calculated (≈500 keV, depending on the energy), and was taken into account in the analysis to obtain 'effective' beam energies.

The fusion-evaporation residues (ER) were detected at 0° and at small angles by using the electrostatic deflector [21] in use at LNL. Most of the beam and beam-like particles were separated out and stopped before entering the detector telescope consisting of two microchannel plate (MCP) detectors, a transverse-field ionization chamber (IC) filled with CH_4, and a 600 mm^2 silicon (Si) detector placed in the back of the IC. The ER were identified by the two independent time-of-flights Si-MCP, by the energy loss ΔE in the IC and by the residual energy provided by the Si detector. The transmission of the electrostatic deflector was estimated to be 0.45 ± 0.02 from previous measurements for systems with similar mass asymmetries, and confirmed by Monte Carlo calculations. Four monitor detectors were placed at $\theta \simeq 16°$, symmetrically around the beam direction.

The excitation function was measured at $\theta_{lab} = 2°$ in a sequence of runs starting from the highest nominal energy 125 MeV. The ER angular distribution was measured at $E_{lab} = 125$ and 109 MeV in the range $-7°$ to $+7°$ with steps of one degree. Figure 2 shows the measured distribution at 109 MeV where the statistics is better. The energy dependence of the width and shape of the angular distribution is expected to be very small in the energy range of the excitation function, and this is what we have actually observed (as in several previous experiments on near-barrier fusion). The measured ER angular distribution for ^{28}Si + ^{100}Mo is symmetrical around 0° and drops by a factor ≈25 at 7°.

Fusion–fission is negligible for the present system in the measured energy range, on the basis of calculations using the code PACE4 [22] with standard parameters. Therefore, total fusion cross sections were obtained by integrating the ER angular distributions and by the ER yields normalised to the elastic counts into the monitors. The accuracy of the absolute cross section scale is estimated to be ±7%, (see [21] for more details), where the errors on the transmission of the deflector, on the angular distribution measurement and on the detectors solid angles are taken into account. Statistical uncertainties determine relative errors.

2.2. Short survey of results

All cross sections measured in this work are listed in table 1. The fusion excitation function is shown in figure 1 with full red dots, together with the previous result [15]. It can be observed that the present data have a much more regular behaviour, and in particular the new measurement at $E_{c.m.} = 65.9$ MeV yields a cross section larger by a factor ≃200. Most importantly, this gives a smooth trend to the low-energy part of the excitation function. In the remaining part of this article we shall consider for the analyses only the cross sections derived from the

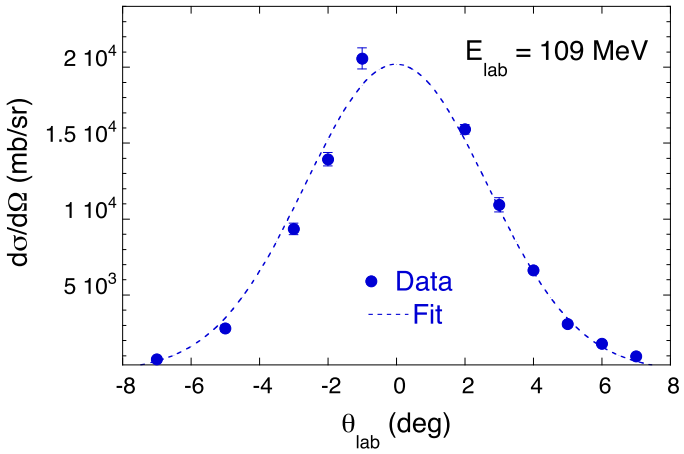

Figure 2. ER angular distribution for ^{28}Si + ^{100}Mo at the beam energy 109 MeV. The dashed line is the Gaussian fit used to obtain the total fusion cross section.

Table 1. Fusion cross sections measured in this work for ^{28}Si + ^{100}Mo (see text). The quoted errors are statistical uncertainties.

$E_{\rm c.m.}$ (MeV)	σ (mb)	Error (mb)
65.20	0.034	0.014
65.95	0.215	0.031
67.50	1.04	0.18
68.40	3.42	0.44
71.44	23.8	2.1
72.90	38.4	6.3
74.50	68.4	11.2
77.80	149.5	13.6
79.19	182.0	29.8
84.80	375.4	28.8
89.80	574.0	93.0
91.50	612.0	100.0
97.30	790.0	80.0

present experiment. They are reported also in figure 3(a) together with the CC calculations we are going to describe in the following section. Panel (b) shows the astrophysical S factor.

3. Coupled-channels analysis

The CC program CCFULL [9] has been employed for the theoretical analysis of the present data on ^{28}Si + ^{100}Mo. In CCFULL the number of CC equations is reduced by means of the isocentrifugal approximation, and an incoming-wave boundary condition (IWBC) [26] is placed inside the barrier. The effects of inelastic non-linear couplings are included to all orders, and full account is taken of the finite excitation energies of the coupled modes. Vibrational couplings are treated in the harmonic limit, and rotational coupling with a pure rotor. CCFULL

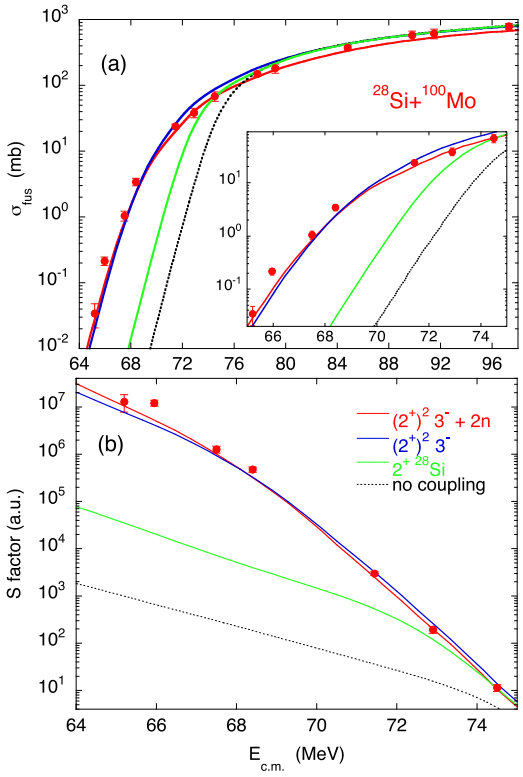

Figure 3. Excitation function (a) and astrophysical *S* factor (b) measured in the present work (red full dots), compared to CC calculations (see text for details).

includes a pair-transfer coupling between the ground states, by using the macroscopic coupling form factor given by Dasso and Pollarolo [10].

The Woods Saxon ion–ion potential used for the CC calculations has well depth $V_0 = 75.1$ MeV, diffuseness $a = 0.66$ fm and radius parameter $r_0 = 1.15$ fm. V_0 is deeper than the Akyüz–Winther potential [27] ($V_0 = 68.3$ MeV, $a = 0.66$ fm and $r_0 = 1.18$ fm for the present system). This choice avoids oscillations in the transmission coefficients of high partial waves, especially at energies above the Coulomb barrier, appearing if the potential is too shallow, because of an incorrect application of the IWBC.

The diffuseness has not been changed, while the radius parameter has been adjusted so to obtain a good data fit in the barrier region $\sigma = 10$–100 mb, when all channels, including the two-nucleon transfer (see later on) are taken into account. The nuclear structure information on the low-lying collective modes of ^{28}Si and ^{100}Mo is reported in table 2.

3.1. The excitation function

Figure 3(a) shows the results of the calculations when compared to the present experimental data (full red dots). We first notice that the sub-barrier cross section enhancement is very large with respect to the no coupling limit (more than a factor 700, dashed black line). Including in the coupling scheme the lowest three members of the ground state rotational band of the oblate ^{28}Si, produces already a rather large effect (green line). The octupole vibration is very high

Table 2. Excitation energies E_x, spin and parities λ^π, and deformation parameters β_λ [23, 24] of the lowest quadrupole and octupole modes of ^{28}Si and^{100}Mo, and of the other nuclei involved in the comparison of section 4. The β_λ values have been estimated using the radius parameter $r_0 = 1.20$ fm. Nuclear and Coulomb deformation parameters have been taken to be the same. The β_2 parameter for ^{28}Si is negative, given the oblate deformed shape [25] of that nucleus.

Nucleus	E_x (MeV)	λ^π	β_λ
^{28}Si	1.779	2^+	−0.41
	6.879	3^-	0.40
^{100}Mo	0.536	2^+	0.23
	1.908	3^-	0.22
^{32}S	2.230	2^+	0.31
	5.006	3^-	0.54
^{96}Zr	1.751	2^+	0.08
	1.897	3^-	0.29
^{90}Zr	2.186	2^+	0.09
	2.748	3^-	0.21

(see table 2), its adiabatic effect is already included in the adjustment of the ion–ion potential, and consequently the 3^- state has not been considered in the CC calculation.

By including also the vibrational collective mode of ^{100}Mo up to the two-phonon level (the 2^+ state is very low, at 0.536 MeV), we obtain the blue curve in the figure. The excitation function is rather well reproduced, apart from small disagreements near and far below the barrier. There is little difference from the calculations including only one phonon. The second phonon brings a small additional enhancement at energies below the barrier, and a third phonon has a negligible effect. The results of one- and three-phonon calculations are not reported in the figure for clarity of presentation. For ^{100}Mo the 3^- excitation has been explicitly considered, because it is rather low in energy, albeit not so strong.

At this point, we have performed further calculations, including the two neutron transfer channel ($+2n$) besides the collective surface modes discussed here above, using the approximate treatment of CCFULL for transfer couplings. The ground state Q-value for two-neutron pick up from ^{100}Mo to ^{28}Si is $Q = +4.86$ MeV. The coupling strength $F_t = 0.5$ MeV has been used, adjusted to optimize the data fit.

A smaller F_t results in a negligible overall effect, while a larger coupling strength produces an increasing data under-prediction above the barrier (as expected). Anyway, it appears that transfer coupling does not produce a large effect in the present system, see again figure 3(a), in spite of the large positive Q-value for two-neutron pick up. This is probably so, because the largest effect on sub-barrier cross sections is due to the strong quadrupole vibration of ^{100}Mo and to the deformed structure of ^{28}Si. In this sense, the behaviour of ^{28}Si + ^{100}Mo in the sub-barrier region parallels the excitation function of ^{60}Ni + ^{100}Mo [18] that was found to be dominated by the multi-phonon excitations of the strong quadrupole vibration of the common target ^{100}Mo.

We would like to point out the quantum diffusion approach of references [19, 20], which was applied to study the fusion dynamics where deformed and spherical nuclei are involved. The small effect of transfer channels in ^{28}Si + ^{100}Mo may be related to the fact that after the two-neutron transfer the resulting ^{30}Si is a spherical nucleus and in ^{98}Mo the quadrupole

deformation is weaker and higher in energy. Indeed, the approach of Sargsyan and co-workers, anticipates that the neutron transfer weakly influences the fusion in cases like the present one.

3.2. The astrophysical S factor

Figure 3(b) shows the measured astrophysical S factor for ^{28}Si + ^{100}Mo, compared to the results of the CC calculations. The experimental S factor at the lowest energy show a tendency to become flat. However, we have no indication of a maximum vs energy, and at least one more data point at lower energy would be necessary to decide whether fusion hindrance shows up or not. Actually, the phenomenological systematics of reference [28] predicts the hindrance threshold at ≈66 MeV, close to the lowest measured point at $E = 65.2$ MeV. That systematics was originally developed for stiff systems, it is not unexpected, therefore, that the hindrance threshold for ^{28}Si + ^{100}Mo may appear slightly lower than 66.0 MeV, given the soft vibrational nature of ^{100}Mo.

None of the CC calculations performed with the WS potential is able to reproduce the trend of S. Including the two-neutron coupling yields a slightly better result at the lowest energies. We can imagine that, in order to fit the data, a shallower potential should be used, as the M3Y + repulsion interaction introduced by Esbensen and Mişicu [29, 30], or that one should follow the suggestion of Simenel *et al* [31] that the Pauli exclusion principle gives rise to a short range repulsion in the ion–ion potential. Alternatively, the adiabatic model [32–34] is a successful approach to account for hindrance, where a quenching of the coupling strengths inside the touching point of the two nuclei is introduced. We remark also that the quantum diffusion model mention in the previous section has been recently extended to deep sub-barrier fusion of medium-light and light systems [35]. The hindrance phenomenon has been correctly reproduced in several cases. The application of such theoretical approaches is anyway beyond the scope of this work.

4. Comparison with ^{60}Ni + ^{100}Mo and near-by systems

4.1. The case of ^{60}Ni + ^{100}Mo

The comparison of the present system with ^{60}Ni + ^{100}Mo is interesting because of the common molybdenum target with its strong quadrupole vibrational mode, and in view of the many $Q > 0$ transfer channels existing in that heavier system (see table 3), in close analogy with the case of ^{28}Si + ^{100}Mo. The fusion excitation function of ^{60}Ni + ^{100}Mo was measured a few years ago [18] down to a cross section around 2 μb, looking for coupling and hindrance effects in that soft medium-mass system. It was found that the threshold for fusion hindrance was not reached, and multi-phonon excitations are predominant in the sub-barrier cross section enhancement, originating from the strong quadrupole mode of ^{100}Mo that gives an increasing contribution up to the level of four phonons.

We point out that CCFULL treats vibrational modes in the harmonic limit, and this may not be a good approximation, especially for heavy systems. On the other hand, above the two-phonon level spectroscopic information on the vibrational mode of ^{100}Mo is very limited. With this kind of warnings in mind, anyway, the very nice data fit leaves little space for the possible effect of transfer couplings in ^{60}Ni + ^{100}Mo.

It appears that we find a similar situation in ^{28}Si + ^{100}Mo, as discussed in the previous section. In this lighter system we observe that *two* phonons of the ^{100}Mo vibration, are already 'enough' to reproduce the fusion data, as actually might have been qualitatively expected. Relatively to each other, the two excitation functions are different. They are compared in figure 4, where the quantity $E \times \sigma_{\rm fus}$ is reported vs the energy distance from the barrier evaluated using

Table 3. Ground state Q values (in MeV) of one- to four-neutron pick up reactions for the systems discussed in section 4.

System	Q_{1n}	Q_{2n}	Q_{3n}	Q_{4n}
^{28}Si + ^{90}Zr	−3.50	−2.20	−7.96	−8.97
^{28}Si + ^{96}Zr	+0.62	+4.77	+3.13	+5.60
^{32}S + ^{90}Zr	−3.33	−1.23	−6.59	−6.32
^{32}S + ^{96}Zr	+0.79	+5.74	+4.51	+7.66
^{32}S + ^{100}Mo	+0.35	+5.84	+4.18	+7.25
^{28}Si + ^{100}Mo	+0.18	+4.86	+2.81	+5.19
^{60}Ni + ^{100}Mo	−0.47	+4.20	+2.40	+5.23

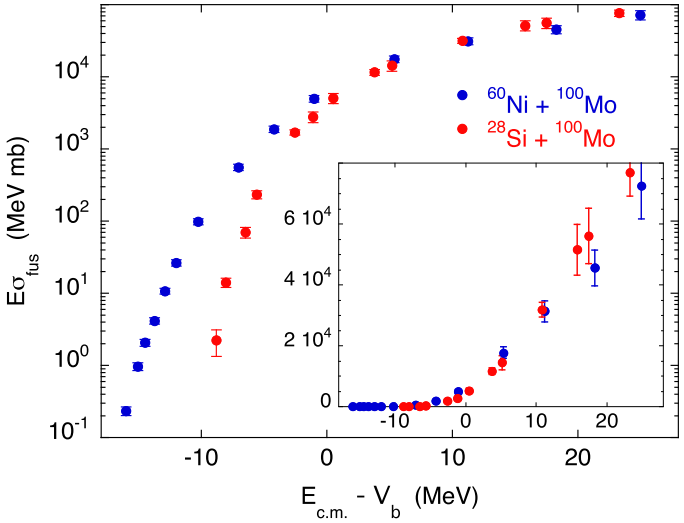

Figure 4. Fusion excitation functions of ^{28}Si + ^{100}Mo and ^{60}Ni + ^{100}Mo [18]. The two energy scales are corrected by taking account of the AW Coulomb barrier for each system.

the AW potential. The inset is the same plot in a linear scale better showing that the energy scale normalisation according to the AW barrier is a good choice, because the data of the two systems essentially coincide above the barrier. However, from the logarithmic plot one immediately realises that the near- and sub-barrier fusion enhancement of the heavier system is much larger. The previous considerations (mainly based on the CC results) lead us to conclude that the difference can be almost entirely ascribed to the multi-phonon excitations of ^{100}Mo.

4.2. The near-by systems and the ion–ion potentials

The sub-barrier fusion of several systems involving nuclei near ^{28}Si and/or ^{100}Mo has been investigated by various groups. We shall consider and comparatively analyse in this section the experimental excitation functions of selected systems, and we shall see to what extent the various observed trends can be linked to different nuclear structure properties, and transfer couplings. We chose to include in this comparison the systems ^{28}Si + ^{90}Zr [36], ^{28}Si + ^{96}Zr

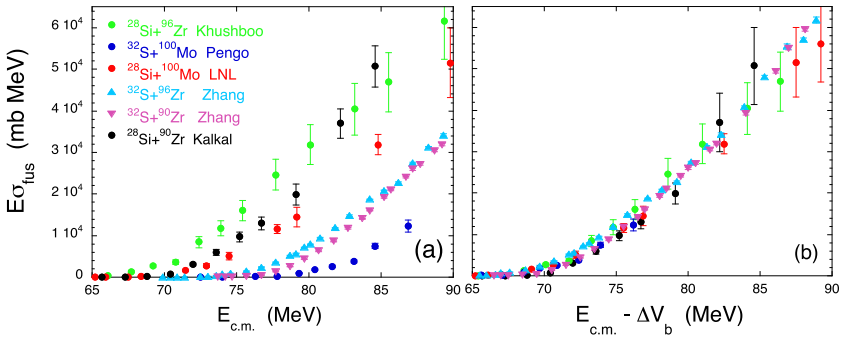

Figure 5. Fusion excitation functions in linear scale of ^{28}Si + ^{100}Mo and of the other systems considered for comparison. The reported systems are ^{28}Si + ^{96}Zr [37], ^{32}S + ^{100}Mo [38], ^{32}S + ^{90,96}Zr [11], ^{28}Si + ^{90}Zr [36], besides ^{28}Si + ^{100}Mo.

[37], ^{32}S + ^{90,96}Zr [11], and ^{32}S + ^{100}Mo [38], besides ^{28}Si + ^{100}Mo that is the object of the present work.

Table 2 reports the nuclear structure information of all involved nuclei. The corresponding neutron transfer Q-values are shown in table 3. The main difference between the two projectiles is that ^{28}Si has a permanent oblate deformation [25] (see previous section), while ^{32}S is a vibrational-like nucleus where, however, the quadrupole mode is rather high in energy (at 2.230 MeV, see table 2). In both cases the octupole state lies above 5 MeV, so that a simple re-normalisation of the ion–ion potential is produced in the coupling [39], without affecting the shape of the barrier distribution and, consequently, of the overall excitation function.

Concerning the Zr and Mo cases, ^{90}Zr is a semi-magic stiff nucleus, ^{96}Zr is characterised by a strong octupole vibration at a relatively low energy, and ^{100}Mo is a strong vibrational nucleus having the quadrupole mode at only 536 keV. All data are taken from references [23, 24].

From the point of view of the transfer couplings on fusion, we can see from table 3 that for the systems ^{28}Si + ^{90}Zr and ^{32}S + ^{90}Zr only pick-up channels with negative Q-values are available, while several large and positive transfer Q-values exist for all other cases.

We show in figure 5(a) the excitation functions of the considered systems, in linear scale. The plotted quantity is $E \times \sigma_{\rm fus}$ vs center-of-mass-energy. The excitation functions are linear above the barrier, according to the classical expression $E\sigma_{\rm fus} = \pi R_{\rm b}^2(E - V_{\rm b})$. Here a direct comparison of the several systems is obviously not possible, because the data are spread around by the different Coulomb barriers. We take account of this in panel (b) of the same figure, where, using the AW potential [27], the energy scales are modified relative to ^{28}Si + ^{90}Zr chosen as reference case. The abscissa for ^{28}Si + ^{90}Zr is not changed, while for each of the other systems it is shifted by the quantity $E - \Delta V_{\rm b}$, where $\Delta V_{\rm b}$ is the difference of the Coulomb barrier with respect to ^{28}Si + ^{90}Zr. An analysis of this kind was performed in reference [40] for various Ca + Zr systems.

Additional small shifts have been applied to the modified energy scale of the systems involving ^{32}S, i.e. +2.2, +1.4 and +1.3 MeV for ^{32}S + ^{90}Zr, ^{32}S + ^{96}Zr and ^{32}S + ^{100}Mo, respectively. Those shifts were determined in the $E - \Delta V_{\rm b}$ region $\simeq$74–78 MeV, corresponding to cross sections $\approx$80–300 mb (above the barrier), in such a way that all excitation functions get as close as possible to each other, and to that of ^{28}Si + ^{90}Zr.

The need for such adjustments may originate from (1) the re-normalisation of the potential due to high-energy modes in some cases (the octupole vibration in ^{32}S is stronger than in ^{28}Si, thus producing lower Coulomb barriers), and (2) possible differences in the beam energy and/or

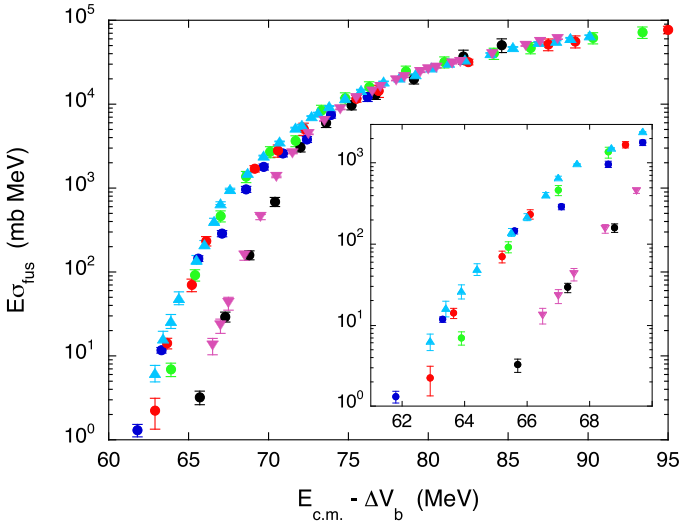

Figure 6. Fusion excitation functions of the same systems of figure 5. Here the cross section scale is logarithmic, and the inset shows the detail of the low-energy part. The symbols for the various systems are the same as in figure 5.

in the absolute cross section scales owing to the fact that the experiments were performed at various accelerators, and using different set-ups. In any case we point out that the AW potential [27] was proposed to fit the experimental data of many heavy-ion systems, so that variations of the parameters for near-by systems having different nuclear structure properties are not unexpected, especially if strong collective modes are involved, as in some of the cases we are analysing.

4.3. Comparison and discussion

The excitation functions resulting from correcting for the different AW barriers and from the small additional energy shifts are shown in figure 5(b). We notice first that the excitation function of ^{28}Si + ^{90}Zr (and of ^{32}S + ^{90}Zr at the highest energies) rises more rapidly than the others, even if all excitation functions obviously approximately coincide in the reference region $\simeq$74–78 MeV (please note the linear scale). Lower above-barrier cross sections are indeed expected in the CC model for the systems where several $Q > 0$ transfer channels exist (see e.g. figure 4(b) of reference [8]). This is so also for ^{28}Si + ^{100}Mo, while for ^{32}S + ^{100}Mo the data do not extend high enough in energy to come to a conclusion.

The same data shown in figure 5(b) are plotted in figure 6 in logarithmic scale. The low-energy part of the excitation function is reported in the inset, in more detail. Here we see that the excitation functions of the two systems involving ^{90}Zr, that is ^{28}Si,^{32}S + ^{90}Zr, almost coincide with each other near and below the barrier. This originates from the potential adjustments we have applied above the barrier, which well 'compensate' for the different structure of ^{28}Si and ^{32}S, and from the fact that both systems have only large negative Q-values for neutron transfer.

All other cases are gathered in a well separated group below the barrier, with relatively small differences between the various systems. For all of them several $Q > 0$ pick-up channels exist (see table 3). However, we cannot conclude that transfer couplings fully explain the situation appearing from figure 6. Indeed, we have seen the CC results for ^{28}Si + ^{100}Mo in section 3

where most of the cross section enhancement is calculated to come from the strong quadrupole vibration of ^{100}Mo (besides the coupling to the rotational states of ^{28}Si). It is reasonable to guess that this happens for ^{32}S + ^{100}Mo as well.

For the other two systems ^{28}Si, ^{32}S + ^{96}Zr $Q > 0$ transfer couplings may also be important. On the other hand, a strong enhancement may be produced by the strong (and relatively low) octupole vibration of ^{96}Zr (see table 2). This was already observed in the comparison of the various Ca + Zr systems carried out in reference [40], see figure 1(d).

Apart from the case of ^{28}Si + ^{100}Mo that we have analysed in some detail in section 3, it is hard, for the other systems, to disentangle, from the comparison of the excitation functions only, the concurring effects of collective vibrational modes from the possible influence of $Q > 0$ transfer channels. A step further would be done by comparing the various BD, as it was done in the original papers reporting the experiments on ^{28}Si + ^{90,96}Zr [11]. For the other cases, however, the excitation functions available in the literature do not have sufficiently small energy steps and high statistical accuracy, so to allow extracting meaningful BD [7]. This is so also for ^{28}Si + ^{100}Mo, where the new data points whose measurement has been reported in this article are relatively few, and spread in a rather wide energy range. The need for CC calculations where (multi)-nucleon transfer couplings can be explicitly included, is also strongly felt.

5. Summary and conclusions

The fusion excitation function of the system ^{28}Si + ^{100}Mo near and below the Coulomb barrier has been measured in a new experiment, because previous data show some irregular behaviors, and the cross section at the lowest energy appears to be unreasonably small. The present data show an overall trend smoother than in the previous experiment, and in particular a large discrepancy is found for the lowest-energy region, since the present excitation function is a factor $\approx$200 larger than the previous result.

CC calculations have been performed using the code CCFULL, including the low-energy excitation modes of both nuclei. The agreement with data is good, when the three lowest rotational excitations of ^{28}Si, and two-phonons of the strong quadrupole vibration of ^{100}Mo are considered. A negligible further enhancement is obtained if three phonons of the quadrupole vibration are included. Several neutron transfer channels with $Q > 0$ exist, in particular the two-neutron pick-up between ground states has a large and positive Q-value = +4.86 MeV, however, schematically coupling this additional channel in CCFULL has a minor effect on the calculated cross sections, and the data fit is not essentially improved. The analogy with the case of the heavier system ^{60}Ni + ^{100}Mo [18] has been highlighted. In that case four phonons of the collective mode of ^{100}Mo have to be considered for a good data fit, while the influence of transfer couplings was found to be of minor importance, as for ^{28}Si + ^{100}Mo.The present data do not allow locating the hindrance threshold which is probably pushed down in energy by the strong rotational and vibrational couplings. It would be interesting to perform further calculations within the quantum diffusion approach [35] that has demonstrated to be able to describe the hindrance effect in several cases.

In the last part of this work, we have compared the excitation function of ^{28}Si + ^{100}Mo and the published data of several near-by ^{28}Si, ^{32}S + Zr, Mo systems where different nuclear structure situations and transfer Q-values are found. This mass region is interesting because of the existence of strong octupole (^{96}Zr) and quadrupole (^{100}Mo) collective modes, of the neutron shell closure at $N = 50$ and the consequent semi-magic nature of ^{90}Zr, and of large positive neutron transfer Q-values for several of the considered systems.

The comprehensive comparison contributes to clarify how all such features influence fusion cross sections near and below the Coulomb barrier, even if the concurring effect of different

modes does not allow to recognize their relative importance in many cases, by only this simple, yet detailed, comparison of the various excitation functions. The need of more systematic experiments dedicated to the extraction of fusion BD is evident, as well as of CC calculations able to accurately include transfer couplings, in order to take further steps to clarify the physics underlying heavy-ion sub-barrier fusion in the considered mass range.

Acknowledgments

We would like to thank K Hagino for helpful discussions on the topics investigated in the present article. We gratefully acknowledge the participation of L Corradi, E Fioretto, D Guarrera, F Scarlassara, G Jaworski, E Strano and I Zanon in part of the measurements. The XTU Tandem staff provided us with high quality beams and M Loriggiola prepared targets of excellent quality. The research leading to these results has received funding from the European Union Seventh Framework Program FP7/2007–2013 under Grant Agreement No. 262010-ENSAR.

Data availability statement

The data that support the findings of this study are available upon reasonable request from the authors.

ORCID iDs

A M Stefanini https://orcid.org/0000-0002-1207-8273
G Montagnoli https://orcid.org/0000-0002-8944-1456
C Dehman https://orcid.org/0000-0003-0554-7286
R Somasundaram https://orcid.org/0000-0003-0427-3893
V Vijayan https://orcid.org/0000-0002-4690-2515

References

[1] Back B B, Esbensen H, Jiang C L and Rehm K E 2014 *Rev. Mod. Phys.* **86** 317
[2] Dasgupta M, Hinde D J, Rowley N and Stefanini A M 1998 *Annu. Rev. Nucl. Part. Sci.* **48** 401
[3] Montagnoli G and Stefanini A M 2017 *Eur. Phys. J.* A **53** 169
[4] Broglia R A, Dasso C H, Landowne S and Winther A 1983 *Phys. Rev.* C **27** 2433
[5] Dasso C H, Landowne S and Winther A 1983 *Nucl. Phys.* A **407** 221
[6] Dasso C H, Landowne S and Winther A 1983 *Nucl. Phys.* A **405** 381
[7] Rowley N, Satchler G R and Stelson P H 1991 *Phys. Lett.* B **254** 25
[8] Esbensen H, Stefanini A M and Montagnoli G 2016 *Phys. Rev.* C **93** 034609
[9] Hagino K, Rowley N and Kruppa A T 1999 *Comput. Phys. Commun.* **123** 143
[10] Dasso C H and Pollarolo G 1985 *Phys. Lett.* B **155** 223
[11] Zhang H Q *et al* 2010 *Phys. Rev.* C **82** 054609
[12] Jia H M *et al* 2016 *Phys. Lett.* B **755** 43
[13] Zagrebaev V I 2003 *Phys. Rev.* C **67** 061601(R)
[14] Karpov A V, Rachkov V A and Samarin V V 2015 *Phys. Rev.* C **92** 064603
[15] Ackermann D *et al* 1995 *Nucl. Phys.* A **583** 129
[16] Jiang C L *et al* 2002 *Phys. Rev. Lett.* **89** 052701
[17] Jiang C L *et al* 2004 *Phys. Rev. Lett.* **93** 012701
[18] Stefanini A M *et al* 2013 *Eur. Phys. J.* A **49** 63

[19] Sargsyan V V, Adamian G G, Antonenko N V, Scheid W and Zhang H Q 2011 *Phys. Rev.* C **84** 064614
[20] Sargsyan V V, Adamian G G, Antonenko N V, Scheid W and Zhang H Q 2012 *Phys. Rev.* C **85** 024616
[21] Stefanini A M *et al* 2010 *Phys. Rev.* C **82** 014614
[22] Gavron A 1980 *Phys. Rev.* C **21** 230
[23] Raman S, Nestor C W Jr and Tikkanen P 2001 *At. Data Nucl. Data Tables* **78** 1–128
[24] Kibédi T and Spear R H 2002 *At. Data Nucl. Data Tables* **80** 35
[25] Stone N J 2005 *At. Data Nucl. Data Tables* **90** 75
[26] Esbensen H 2003 *Phys. Rev.* C **68** 034604
[27] Akyüz Ö and Winther Å 1981 Nuclear structure and heavy-ion physics *Proceedings of the International School of Physics 'Enrico Fermi' Course LXXVII Varenna* ed R A Broglia and R A Ricci (Amsterdam: North Holland)
[28] Jiang C L, Rehm K E, Back B B and JanssensR V F 2009 *Phys. Rev.* C **79** 044601
[29] Mişicu Ş and Esbensen H 2006 *Phys. Rev. Lett.* **96** 112701
Mişicu Ş and Esbensen H 2007 *Phys. Rev.* C **75** 034606
[30] Esbensen H and Mişicu Ş 2007 *Phys. Rev.* C **76** 054609
[31] Simenel C, Umar A S, Godbey K, Dasgupta M and HindeD J 2017 *Phys. Rev.* C **95** 031601(R)
[32] Ichikawa T, Hagino K and Iwamoto A 2007 *Phys. Rev.* C **75** 057603
[33] Ichikawa T, Hagino K and Iwamoto A 2009 *Phys. Rev. Lett.* **103** 202701
[34] Ichikawa T 2015 *Phys. Rev.* C **92** 064604
[35] Sargsyan V V, Adamian G G, Antonenko N V and Lenske H 2020 *Eur. Phys. J.* A **56** 19
[36] Sunil K *et al* 2010 *Phys. Rev.* C **81** 044610
[37] Khushboo *et al* 2017 *Phys. Rev.* C **96** 014614
[38] Pengo R, Evers D, Löbner K E G, Quade U, Rudolph K, Skorka S J and Weidl I 1983 *Nucl. Phys.* A **411** 255
[39] Hagino K, Takigawa N, Dasgupta M, Hinde D J and Leigh J R 2014 *Phys. Rev. Lett.* **79** 2014–7
[40] Stefanini A M *et al* 2007 *Phys. Rev.* C **76** 014610